

Article

Calculating Economic Flood Damage through Microscale Risk Maps and Data Generalization: A Pilot Study in Southern Italy

Gianna Ida Festa ¹, Luigi Guerriero ², Mariano Focareta ³, Giuseppe Meoli ³, Silvana Revellino ⁴,
Francesco Maria Guadagno ¹ and Paola Revellino ^{1,*}

¹ Department of Sciences and Technologies, University of Sannio, 82100 Benevento, Italy; gidafesta@unisannio.it (G.I.F.); guadagno@unisannio.it (F.M.G.)

² Department of Earth Sciences, University of Naples “Federico II”, 80132 Napoli, Italy; luigi.guerriero2@unina.it

³ MAPSat s.r.l., 82100 Benevento, Italy; m.focareta@mapsat.it (M.F.); g.meoli@mapsat.it (G.M.)

⁴ Department of Management & Innovation Systems, University of Salerno, 84084 Fisciano, Italy; srevellino@unisa.it

* Correspondence: paola.revellino@unisannio.it

Abstract: In recent decades, floods have caused significant loss of human life as well as interruptions in economic and social activities in affected areas. In order to identify effective flood mitigation measures and to suggest actions to be taken before and during flooding, microscale risk estimation methods are increasingly applied. In this context, an implemented methodology for microscale flood risk evaluation is presented, which considers direct and tangible damage as a function of hydrometric height and allows for quick estimates of the damage level caused by alluvial events. The method has been applied and tested on businesses and residential buildings of the town of Benevento (southern Italy), which has been hit by destructive floods several times in the past; the most recent flooding occurred in October 2015. The simplified methodology tries to overcome the limitation of the original method—the huge amounts of input data—by applying a simplified procedure in defining the data of the physical features of buildings (e.g., the number of floors, typology, and presence of a basement). Data collection for each building feature was initially carried out through careful field surveys (FAM, field analysis method) and subsequently obtained through generalization of data (DGM, data generalization method). The basic method (FAM) allows for estimating in great detail the potential losses for representative building categories in an urban context and involves a higher degree of resolution, but it is time-consuming; the simplified method (DGM) produces a damage value in a shorter time. By comparison, the two criteria show very similar results and minimal differences, making generalized data acquisition most efficient.

Keywords: damage; urban areas; flood risk; GIS; southern Italy



Citation: Festa, G.I.; Guerriero, L.; Focareta, M.; Meoli, G.; Revellino, S.; Guadagno, F.M.; Revellino, P. Calculating Economic Flood Damage through Microscale Risk Maps and Data Generalization: A Pilot Study in Southern Italy. *Sustainability* **2022**, *14*, 6286. <https://doi.org/10.3390/su14106286>

Academic Editors: Stefano Morelli, Veronica Pazzi and Mirko Francioni

Received: 20 April 2022

Accepted: 18 May 2022

Published: 21 May 2022

Publisher’s Note: MDPI stays neutral with regard to jurisdictional claims in published maps and institutional affiliations.



Copyright: © 2022 by the authors. Licensee MDPI, Basel, Switzerland. This article is an open access article distributed under the terms and conditions of the Creative Commons Attribution (CC BY) license (<https://creativecommons.org/licenses/by/4.0/>).

1. Introduction

It is well known that, in the Anthropocene epoch, human activities have affected geological forces in ways that disrupt the usual human–nature relationship [1,2]. For example, the risk associated with flooding events is often increased by the disproportionate and irrational use of highly hazardous areas [3]. It is also true that climate change is playing a significant role in intensifying the extreme hydrological events responsible for severe flooding (e.g., [4–7]). Therefore, the combined action of climate change and human activity increases the fragility of the whole anthropized system (e.g., [8–10]).

As a matter of the fact, the most extreme alluvial events that occurred in recent years were caused by intense and short- to mid-term rainfall (e.g., [11–13]) and were characterized by water flows higher than those generally safely disposed of by the collection systems [14]. It must also be emphasized that these events often require substantial funding for the reconstruction of damaged structures and assets [15–17].

According to the 2007/60/EC directive, correct environmental and territorial planning and a careful evaluation of the hydrogeological risk are needed to guarantee a high level of environmental protection. Accurate land planning also reduces problems connected with the physical transformations of the territory [18–20].

Flood risk assessments are often arranged at a macroscale (e.g., regional level with common detail; see [21]) or at a mesoscale (e.g., municipal level with large mesh raster mapping; see [22,23]), with a resolution of detail that could be too generic to be suitable for local analyses [24]. Conversely, studies focused on microscale methodologies (e.g., [8,25–28]), which consider flood damage as a function of the hydrometric height, can be used to evaluate the risk level of every building in a town.

However, a major limitation of microscale approach methodologies is the collection of data on urban asset characteristics (building and commercial activities), which is the basis for the evaluation of the economic value of the structures at risk. Despite the large amount of data provided by online databases, microscale approaches imply the need for time-consuming on-site inspections to obtain full information on the features of assets that can be damaged.

This paper analyzes the direct and tangible effects of flooding in the town of Benevento, in southern Italy, for all types of assets at risk, and provides a quantitative value for the economic damage through the application of microscale methods existing in the literature. At the same time, it proposes a more simplified and rapid data acquisition method, based on data generalizations that allow the damage level caused by alluvial events to be quickly estimated. This overcomes the limitations to which microscale risk analyses are subject. The results obtained are compared to evaluate whether the data simplification method may return comparable outcomes in terms of risk quantification to those obtained using traditional methods.

With the final aim of providing exploitable flood risk maps, this study uses data related to the historical flooding that occurred in the province of Benevento from previous studies [29–32]; furthermore, hazard levels are deduced from alluvial hazard maps of the Benevento province [33,34], designed to provide easy-to-understand information on the annual probability of flooding on the major river segments. The analysis provides new and useful perspectives on current flood risk assessment across Benevento.

2. Materials and Methods

2.1. Study Area

The urban and suburban areas of Benevento are located at the confluence of the Calore and Sabato Rivers, which are the main morphogenetic agents of the area (Figure 1). Peculiar landforms detectable in the historical downtown consist of terraced surfaces that connect with the two large alluvial plains of the aforementioned waterways.

Due to this morphological configuration, Benevento and the surrounding area suffered significantly from flooding. The most recent overflow of the Calore River and some of its tributaries occurred on 14–15 October 2015, hitting Benevento and the central part of its province. The intense meteorological event (maximum intensity of 27.4 mm/10 min and maximum cumulative rainfall of 415.6 mm recorded in 19 h at the rain gauge at Paupisi, about 12 km from Benevento) caused two casualties and multiple ground effects, such as flooding, soil erosion, and landslides over wide areas [31,32,35,36]. Estimates of the Campania Region Authority and Italian Farmer Confederation computed damage to buildings, infrastructure, and local agriculture at 700 million and 1 billion Euros, respectively.

As reported in several studies (e.g., [37–40]), this event had dozens of historical precedents in the area. About 15 overflows of the Calore and Sabato Rivers are documented from the last 100 years (Figure 2), some of them with disastrous consequences, including the destructive flooding that occurred in October 1949, when the Calore River caused huge damage to properties and 20 fatalities [32,33,41].

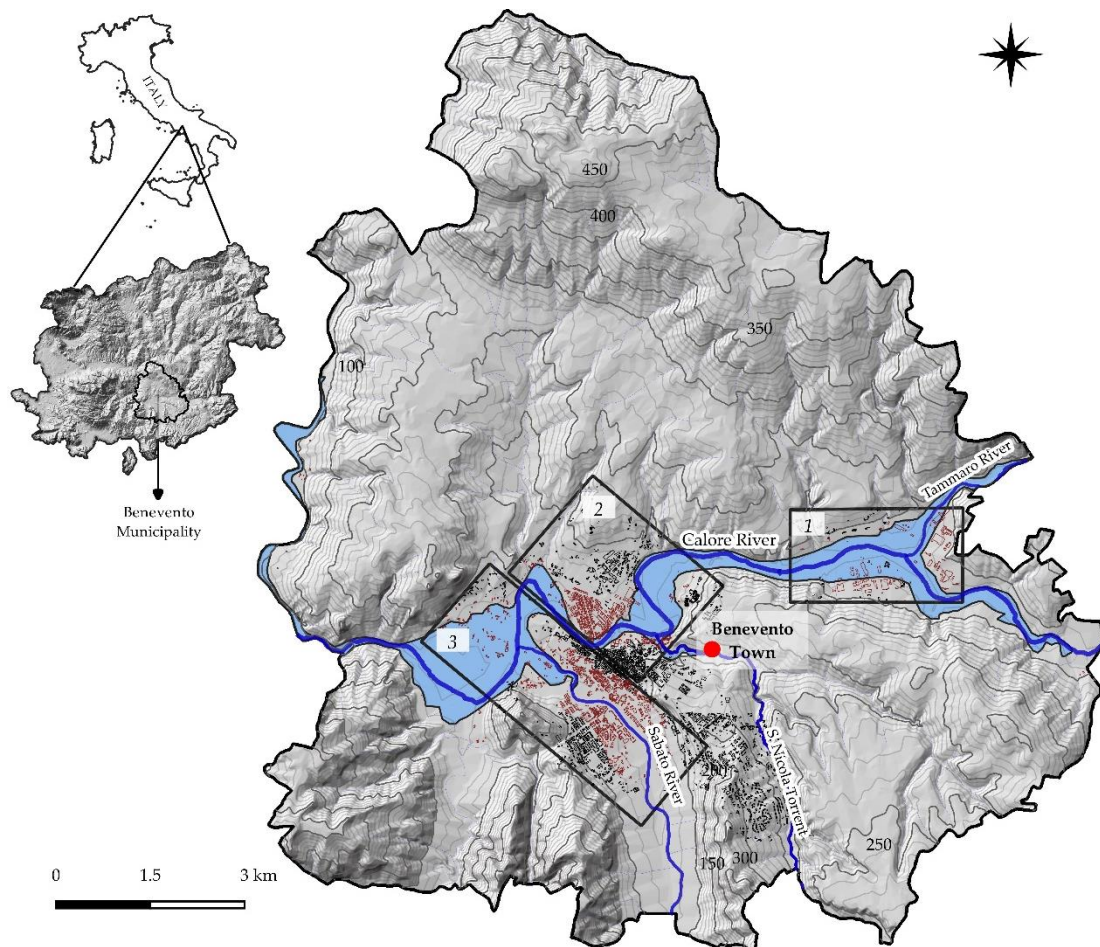


Figure 1. Administrative boundaries of the municipality of Benevento. Black rectangles demarcate the study areas: (1) Industrial area, (2) “Rione Ferrovia” area, and (3) “Rione Libertà” area. The buildings investigated are in red. Overflow of October 2015 of the Calore River is shown in light blue.

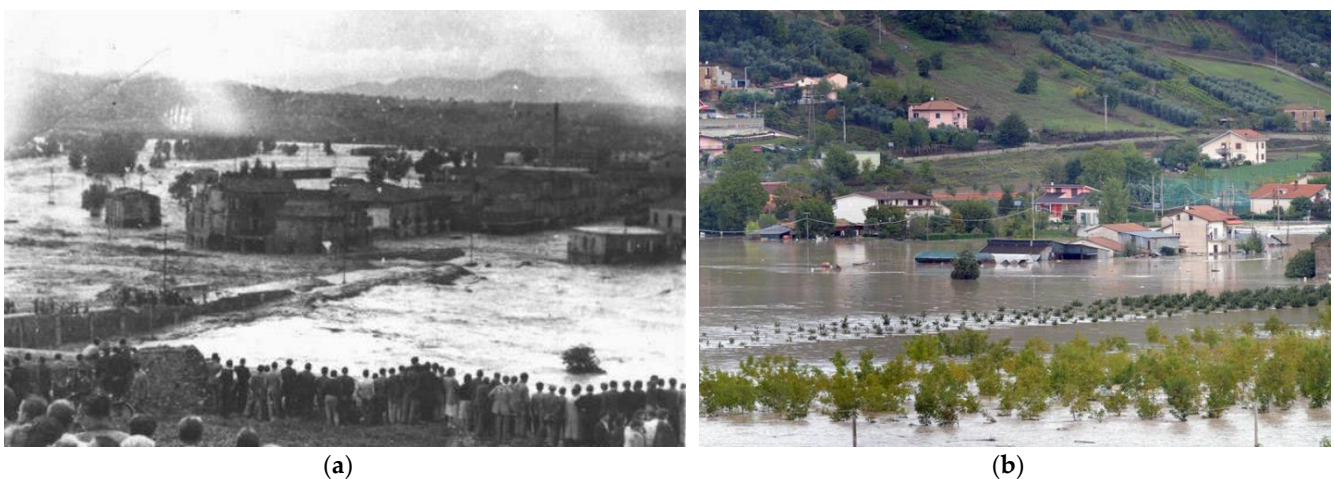


Figure 2. “Rione Ferrovia” area (part of sector 2, Figure 1) flooded in October 1949 (available at https://napoli.repubblica.it/cronaca/2015/10/15/foto/benevento_1_alluvione_del_1949-125118463/1/ (accessed on 12 May 2022) (a), overflow of October 2015 of the Calore River (photo: P. Revellino) (b).

From this historical evidence, it is clear that alluvial phenomena recur in the town of Benevento, which makes a highly accurate assessment of the connected risk essential.

In order to perform flood risk assessment across Benevento, the study area was divided into three sectors (Figure 1), (1) Industrial area, (2) Rione Ferrovia area, and (3) Rione Libertà area. The three sectors are quite different in terms of the building types, as the Industrial area is mainly characterized by industrial warehouses, the Rione Libertà area is a popular neighborhood characterized by residential settlements, and the Rione Ferrovia area has a prevalence of buildings used for commercial purposes.

2.2. Methods

As is well known, the disaster risk connected to the occurrence of natural events is generally defined by the following equation [42,43]:

$$R = H \times V \times E, \quad (1)$$

which expresses the adverse effects suffered by vulnerable people and structures (V = the vulnerability of the exposed elements) and exposed (E = exposure of the elements at risk) as a consequence of the impact of a hazardous event (H = hazard of a natural event).

In the case of flood risk, spatially distributed flood levels and probabilistic time recurrences for events of a given magnitude are usually used for estimate exposure and flood hazard [28,44], whereas vulnerability is assessed by evaluating the potential degree of damage to the exposed elements as a function of the flood water depth estimations.

For the study area, flood risk assessment is based on a step-by-step procedure that uses (i) flood hazard maps from statistical analysis of available hydrometric time series [33]; (ii) two different microscale methods of data collection for the analysis of the features of exposed elements, i.e., buildings; (iii) a model to quantitatively estimate direct and tangible damage; and (iv) an economic analysis.

As regards data collection on features of exposed elements, two different datasets were created using the same type of data (e.g., number of floors, typology, etc.), resulting from a different acquisition method: (1) data derived from scrupulous field analysis, FAM (field analysis method) and, (2) data extracted from the generalization of asset's features, DGM (data generalization method). The two acquisition methods—the first time-consuming and the second more expeditious—should produce two different risk evaluations, which differ in terms of the degree of accuracy and depend on the detail level of the dataset.

Figure 3 is a flowchart of the methodological procedure, whose key steps can be summarized as follows:

- Definition and mapping of flood hazards (hazard, H);
- Definition of elements at risk from both FAM and DGM (exposure, E);
- Definition of the stage–damage curves (vulnerability, V);
- Definition of the building's economic damage;
- Risk estimation (risk, R).

2.3. Hazards

Flood hazard data for the expected damage estimation are (1) the extent of the floodable areas in relation to the main river courses and (2) the value of the relative flood depth [33,34]. Historical data on hydrometric height along the rivers, together with information related to the morphology and topography of the territory, can be used to predict the extent of potentially floodable areas [45–49].

In this study, flood data and hazard maps already available from [33] were used. The authors used high-resolution LiDAR-derived topography and the record of available hydrometric stations along the Calore and Sabato Rivers, from 1924 until 2016, to obtain the annual probability of exceedance for each specific river stage and the return periods. A type III generalized extreme value distribution function (GEV, $\xi < 0$; e.g., [50]) was used to fit the statistical behavior of the annual maximums.

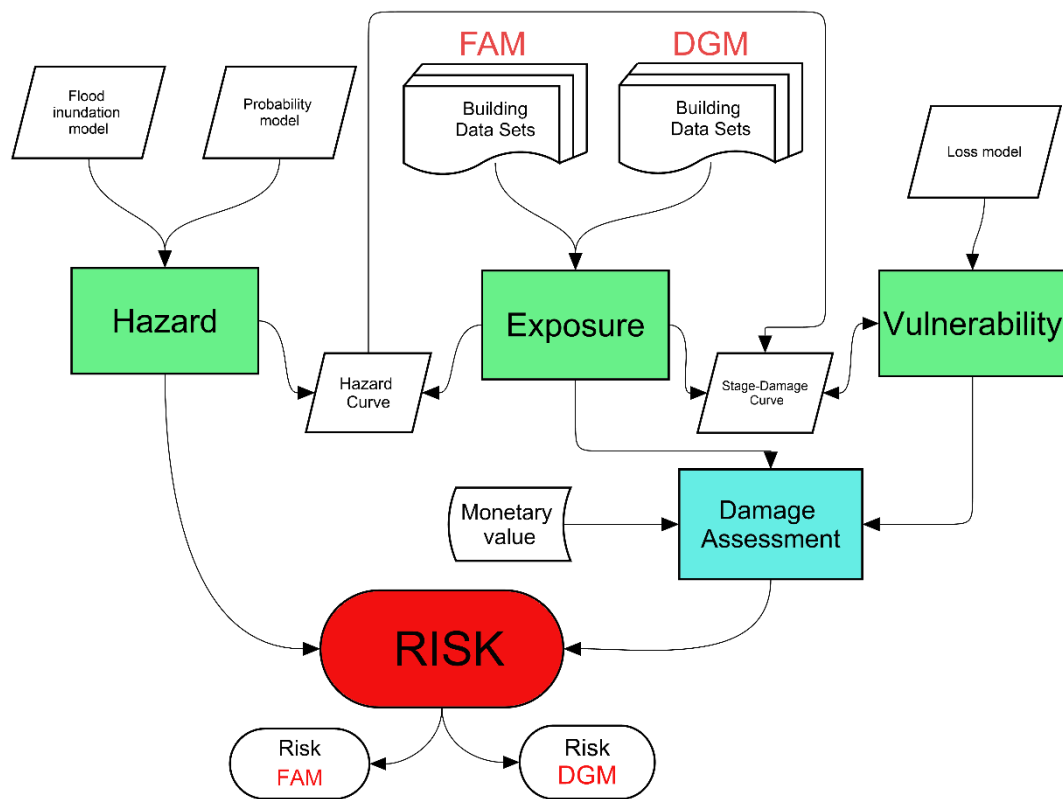


Figure 3. Flowchart of the methodological procedure for microscale flood risk assessments using FAM and DGM building datasets.

The GEV function has the following form:

$$F(x) = \exp \left\{ - \left[1 + \xi \left(\frac{x - \mu}{\sigma} \right) \right]^{-\frac{1}{\xi}} \right\} \text{ for } \xi \neq 0, \quad (2)$$

where ξ , σ , and μ are the shape, scale, and location parameters, respectively.

However, as this function could underestimate the intensity of events with very high return periods, a gamma distribution function [51] was coupled to overcome this limitation, with the form:

$$F(x) = \frac{\beta^\alpha x^{\alpha-1} e^{-\beta x}}{\Gamma(\alpha)}, \quad (3)$$

where α is the shape parameter, β is the scale parameter, and $\Gamma(\alpha)$ is the gamma function, which is calculated as follows:

$$\Gamma(\alpha) = \int_0^x x^{\alpha-1} e^{-x} dx \quad (4)$$

The combined functions were used to derive the flood hazard map as an annual probability of exceedance map and hazard zonation map.

Subsequently, a generic hazard curve for the municipality of Benevento, which can define the hazard level of each human structure located within the floodplains on an annual basis, was derived with respect to the hydrometric zero. The hazard curve was obtained by interpolating the flood depth from the hydrometric zero (sampling step of 0.01 m) and the probability of exceedance (range value between 1 and 0.002, corresponding to a return time of 1 year and 500 years, respectively). For a 500-year return time, the maximum hydrometric height of the watercourse is equal to 14.5 m.

A generic hazard curve was used to define the flood hazard scenarios for each element exposed to risk depending on its position with respect to the watercourse and its height.

2.4. Elements Exposed at Risk

For this study, the area potentially flooded by a 500-year return-time event was considered for identifying and mapping the elements at risk. This choice is consistent with the Italian Ministry of Environment's guidance, which suggests a 300–500-year event be considered as the reference scenario in flood hazard and risk assessment.

Urban buildings of different types and their contents are the elements exposed at risk taken into account for the analysis. For each of them, the following parameters were considered: (1) Type of building; (2) building height from the hydrometric zero (m); (3) building area (m²); (4) number of floors; (5) presence or absence of a cellar; and (6) market value.

Information on the building characteristics were collected by both FAM and DGM methods, resulting in two different datasets. Table 1 summarizes the acquisition criterion for each type of data and method; while building height (2), building area (3), and market value (6) were obtained by the same method, different criteria were used to obtain the type of building (1), number of floors (4), and presence or absence of a cellar (5). Moreover, nine field campaigns for the identification of building characteristics were carried out in the city of Benevento between September and December 2018.

Table 1. Data acquisition criteria.

	Type of Data	FAM ⁽¹⁾	DGM ⁽²⁾
1	Type of building	Field survey	CTR ⁽³⁾
2	Building height (m)	PST ⁽⁴⁾ surveys	PST ⁽⁴⁾ surveys
3	Building area (m ²)	CTR ⁽³⁾ + OSM ⁽⁵⁾	CTR ⁽³⁾ + OSM ⁽⁵⁾
4	Number of floors	Field survey	Building height vs. floor height by category from PST ⁽⁴⁾ surveys
5	Presence of cellar	Field survey	Not considered
6	Market Value (EURm ²)	OMI ⁽⁶⁾	OMI ⁽⁶⁾

⁽¹⁾ Field analysis method. ⁽²⁾ Data generalization method. ⁽³⁾ Regional technical map. ⁽⁴⁾ Not-ordinary plan of remote sensing. ⁽⁵⁾ Open Street Map. ⁽⁶⁾ Real Estate Market Observatory.

(1) The 1:5000 regional technical map (CTR) was used as a topographic basis for preliminary building identification and selection. According to FAM, on-site inspections were performed in order to categorize the building type as residential or commercial. At the same time, all buildings were automatically categorized according to the classification given in the CTR for the DGM dataset. Churches, hospitals, municipalities, and schools were not evaluated in the risk analysis as they can be considered centers for disaster management. During emergencies, these buildings provide temporary accommodation to the affected population; they are locations for strategic, health, and production functions of primary necessity when calamitous events occur [52]. Therefore, being physical assets that fall within the emergency plans, they are not suitable for evaluation with the proposed methodology.

(2) For both FAM and DGM, the building's height in meters was extracted from the DSM (digital surface model) of the PST (Not-ordinary plan of remote sensing) surveys (<http://www.pcn.minambiente.it/mattm/en/not-ordinary-plan-of-remote-sensing/> (accessed on 12 May 2018)) with a 1 × 1 m mesh size. Specifically, the height of each building was assumed to be equal to the 60th percentile of its maximum elevation measured from the ground. This choice was made in order to reduce the effect of the presence of elements, such as chimneys, antennas, and roof gardens, which could cause an overestimation of the building height.

(3) The areas of the buildings (surface in m²) were obtained from the Regional Technical Map (CTR) at a 1:5000 scale of the Campania Region and then controlled, verified, and sometimes integrated using OpenStreetMap (OSM).

(4) Number of floors of each analyzed building were obtained through field analysis, for FAM. As regards DGM, the number of floors was calculated from DSM as the ratio between the building's height and the average height of the floors, according to the building category. To be exact, the average height of a single floor of each building's category was experimentally obtained by measuring the floor height of sample buildings (at least 10 for each category) and computing the average value.

(5) As regards FAM, the presence of a cellar in each building was checked by on-site inspection (the presence of grates or windows near the road surface); conversely, since no data about cellars can be extracted from CTR or OSM, this information was not considered for DGM.

(6) The real estate quote for each building was obtained from the Italian Revenue Agency website (<https://www.agenziaentrate.gov.it/portale/> (accessed on 25 June 2018)) following the categorization provided by the Real Estate Market Observatory (OMI-[53]). The OMI database identifies a minimum and maximum range of market values, per unit area, differentiated for homogeneous area (OMI area) and type of property. It was chosen to consider the average market value for each type of building belonging to the homogeneous OMI area.

The two datasets acquired were incorporated into QGIS; an ID (identifier) was assigned to each building which was correlated with the other information (typology, height, surface, number of floors, cellar, and market value). The following steps were carried out for both datasets.

2.5. Stage–Damage Curves

Damage estimation was performed by assuming a vertical distribution of the economic value of the structure and its contents.

To determine the direct damage from flooding, stage–damage curves were developed that relate the degree of damage to the water height during a flood event [25,54,55]. These curves are different and are functions of the (1) type of building, (2) number of floors, and (3) presence or absence of cellar. They are independent of individual flood events.

Although derived from a simplified analysis, a stage–damage function represents the most suitable model for estimating the direct impact of flooding on buildings. It allows for obtaining a percent loss as a consequence of an event characterized by a specific magnitude and return times. Thus defined, the damage functions have the advantage of being applied to similar urban settings even if geographically distant.

For each floor, the following equation was considered in order to evaluate the percentage degree of damage as a function of the hydrometric height that the building can reach. These equations were used for the stage–damage curves in which the damage, d , is considered as a function of the flood height, h [27]:

$$d_{ki} = d_{ki}(h) \quad (5)$$

where k varies according to the category of building considered (for example, residential, commercial, industrial, etc.), while the parameter i depends on the number of floors and the heights of the floors themselves, which vary according to the category of building itself and therefore to the “ k ” factor, and the presence of a cellar.

2.6. Monetary Damage Estimate

Estimation of the monetary damage was performed for all buildings in the town of Benevento, taking into account representative categories, domestic contents, and commercial activities.

The generic formula, modified from [27], used for the calculation of the total damage (D_{tot}) is:

$$D_{tot} \left(\frac{EUR}{m^2} \right) = D_s + D_c \quad (6)$$

where D_s is the economic damage to the structure only while D_c is the economic damage suffered by the household or business. Here, D_s (the economic loss for a given building, EUR/m^2) is computed as follows:

$$D_s = c \times d_{ki} \times V_s \quad (7)$$

where c is the vulnerability of the building, d_{ki} (%) is the damage percentage associated with the flood depth for each single building, and V_s is the property price (EUR/m^2) calculated for all the floors of a building.

The estate evaluations from the revenue agency consider the conservation status of the buildings and can be used to define a range of values within which the vulnerability parameter c can vary.

The damage, D_c , is defined by the following relationship:

$$D_c = f \times D_s \quad (8)$$

where f is a coefficient that expresses the percentage of the value of the domestic contents as a function of the value in EUR/m^2 of the structure.

2.7. Risk Assessment

The value of the economic loss, defined for a given return time, can be interpolated in the domain of the probability of exceedance to obtain a curve that expresses the risk as EUR/m^2y . This curve is the expected annual damage (EAD), which is the sum of the damage caused by all the floods of any potential magnitude weighted according to the probability of occurrence in a year. The expected annual damage can be computed as follows:

$$Risk = EAD = \int_0^1 D_{tot} \times prob, \quad (9)$$

where “*prob*” is the probability of occurrence for each defined height, i.e., the frequency, for which the total economic damage has been estimated.

Interpolating all data of probability of occurrence for each flood height (with a sampling step of 0.01 m) with the corresponding degree of damage, the flood risk is calculated for each building in $EUR/(m^2y)$. The total risk (EUR/y) for the whole asset can be obtained by multiplying the unitary risk value by its total surface.

To make methodologies and mathematical models replicable for different areas and scales in an automated manner, replacing only the input data, a cross-platform software procedure using Python as the programming language and Postgresql/Postgis as the DBMS (database management system) was developed to store both alphanumeric and geographical input/output data. The input multisource data (see Table 1 and Section 2.5) were normalized, standardized, and verified (i.e., removal of corrupted or redundant data, missing data, etc.) before loading them into the Postgresql database.

Using this software procedure in a cloud environment, it is possible to obtain the risk values for any potentially floodable area with conditions and characteristics comparable to the city of Benevento (10 km^2 —more than 1500 buildings affected) in less than 2 h (with input data already loaded in the DBMS). During the tuning phase of the software procedure, it was found that for an experienced operator the same nonautomated procedure requires at least 6–8 working days.

The results are returned as vectorial data, which contain not only the monetary damage for each single building, but all the basic information extracted and summarized from the input data, such as the building height, number of floors, OMI zone, etc. Vectorial data are thus ready to be imported into a GIS environment, where raster and vectorial data

containing information on flood hazards, building characteristics, stage–damage curves, and monetary damage are used to obtain a spatialized risk map of the study area.

Risk maps, as technologies for managing risks, are important visualization tools that convey information, create awareness, and encourage users to take actions for managing risk [56]. Such graphical representations not only describe the situation but open up new vistas and lead to a new understanding of responsibility and accountability [57].

3. Results

3.1. Hazards

Figure 4 shows the flood hazard maps of the study area resulting from GIS processing and probability analysis [33]. The annual probability of exceedance (Figure 4a) represents the hazard level linked to the occurrence of floods of different magnitudes on an annual basis. The zonation map (Figure 4b) consists of four zones of the study area that can be flooded by events of a specific return period. Accordingly, using the local basin authority guidelines, the four hazard levels chosen are: (i) very high hazard, corresponding to 1–5-year floods; (ii) high hazard, corresponding to 5–30-year floods; (iii) medium hazard, corresponding to 30–100-year floods; and (iv) low hazard, corresponding to 100–500-year floods.

It should be noted that large parts of the floodplain included in the three study areas show high and very high hazard levels. In particular, most of the Industrial area (box 1 in Figure 4), the western sector of Benevento (“Rione Ferrovia” area, box 2 in Figure 4), and the area located along the Sabato River and at the confluence of the Sabato into the Calore River (“Rione Libertà” area, box 3 in Figure 4), are classified as high to very high hazard zones.

3.2. Elements Exposed to Risk

During field surveys, the following information on building features, according to the procedure explained (see Section 2.4), were recorded for a total of 1533 buildings: (1) type of building; (2) building height from hydrometric zero (m); (3) building area (m²); (4) number of floors; (5) presence or absence of a cellar or basement; and (6) market value. As mentioned before, all buildings included within the boundary of a 500-year flood were considered.

Table 2 shows the types of building surveyed and the average floor height computed for each building category. This information was used to derive the number of floors from the total height measured on the DSM, resulting in 1–8-floor buildings. The maps in Figure 5 show different results for buildings’ number of floors from direct field survey (FAM) and computational analysis (DGM).

Using the market value (EUR/m²) of the revenue agency (<https://www.agenziaentrate.gov.it/portale/>, accessed on 1 May 2018), the real estate prices for each building are computed as the average value for each homogeneous OMI zone (OMI zone). The results show that the study area includes five OMI areas with different market values, named (Figure 6): B1, the central area/historic center; B2, the central urban area; C1, the semicentral urban area; C2, the semicentral/“Rione Libertà” area; and, D1, the suburban area/agricultural area. Moreover, within each OMI area, buildings are differentiated by the intended use of the property, distinguishing residential, commercial, productive, and tertiary.

3.3. Stage–Damage Curves

Figure 7 shows the generic flood hazard curve, obtained from a statistical analysis of the hydrometric time series from [33], used to define the hazard levels for each building considered, according to its position with respect to the watercourse and its altimetric characteristics. The generic hazard curve compares the probability of exceedance with the flood depth, for a maximum of 14.5 m from the hydrometric zero corresponding to a 500-year return-time flood and a probability of excess of 0.002. The building height, with respect to the hydrometric zero of the watercourse, is superimposed on the hazard curve

(Figure 7, the red part of the curve) in order to estimate the yearly probability of exceedance of each structure and the portions that can be flooded and damaged.

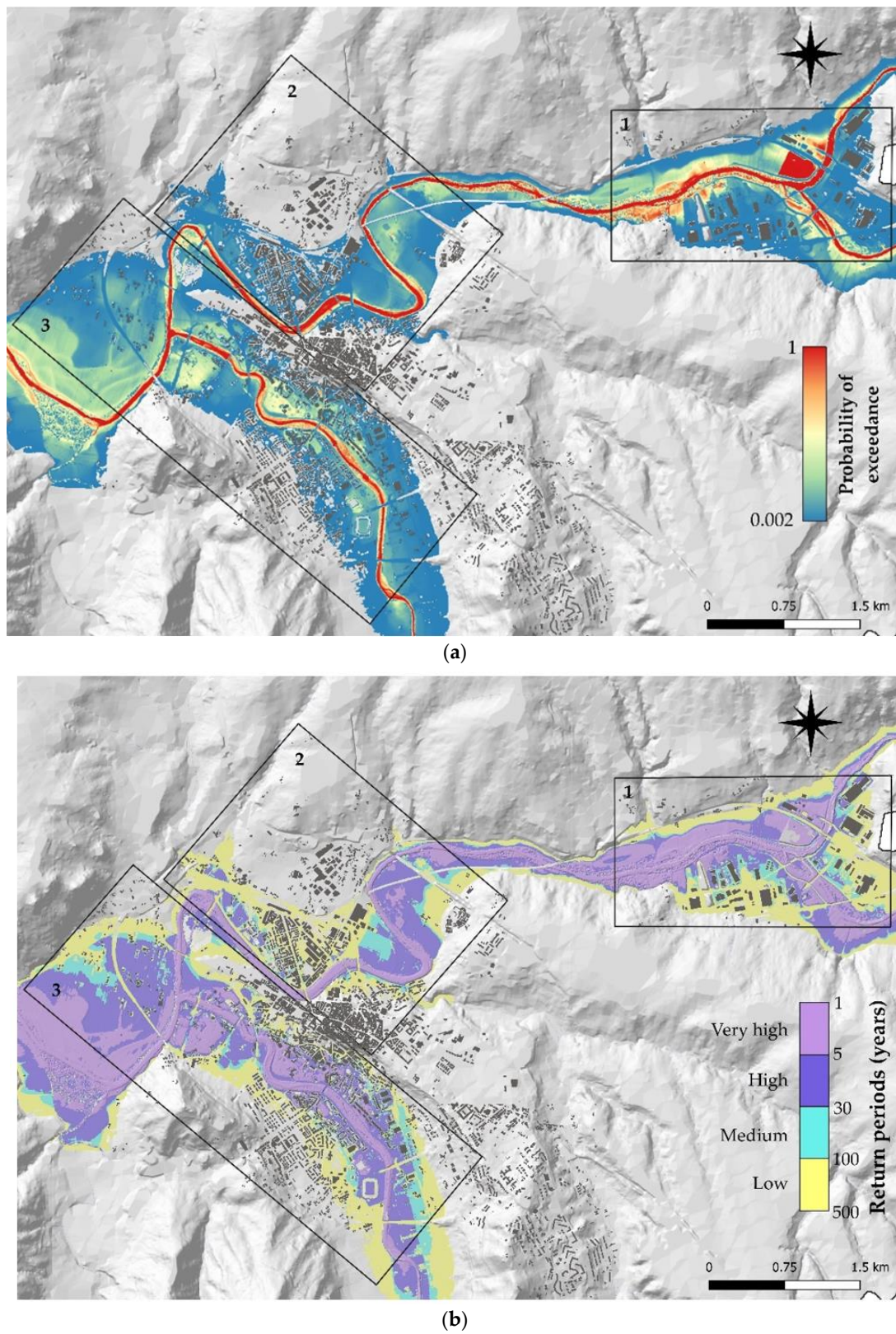


Figure 4. Flood hazard map (a) and flood hazard zonation map (b) of the three selected areas of Benevento (data from [33]).

Table 2. Average height of the building floor for different categories.

Type of Building (FAM and DGM)	Floor Height (m) (DGM)
Civil dwellings, economic housing	3.6
Parking garages, box, villas	3.2
Offices, structured offices	3.7
Industrial sheds, typical warehouses, laboratories	4.5
Shopping centers, stores, shops	4.6
Other	4.3

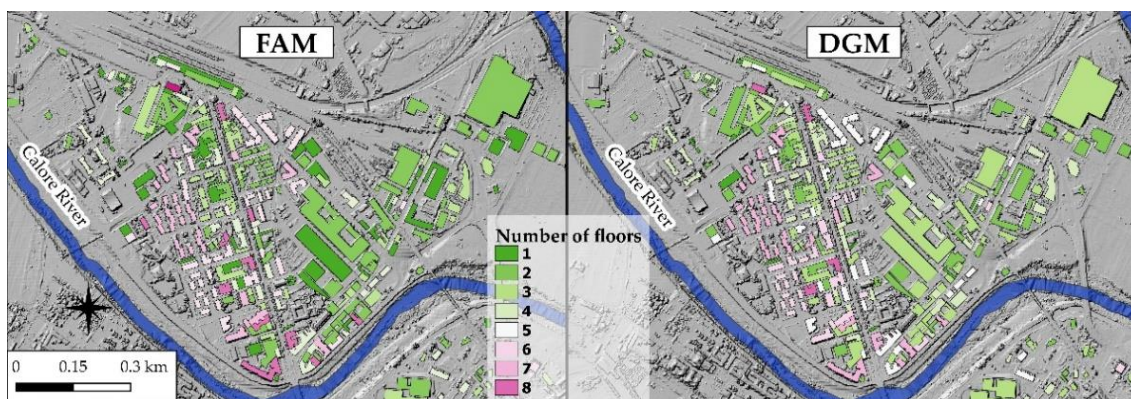


Figure 5. Example of different numbers of floors obtained by surveying (FAM) and computing (DGM) for part of the area #2 “Rione Ferrovia.”

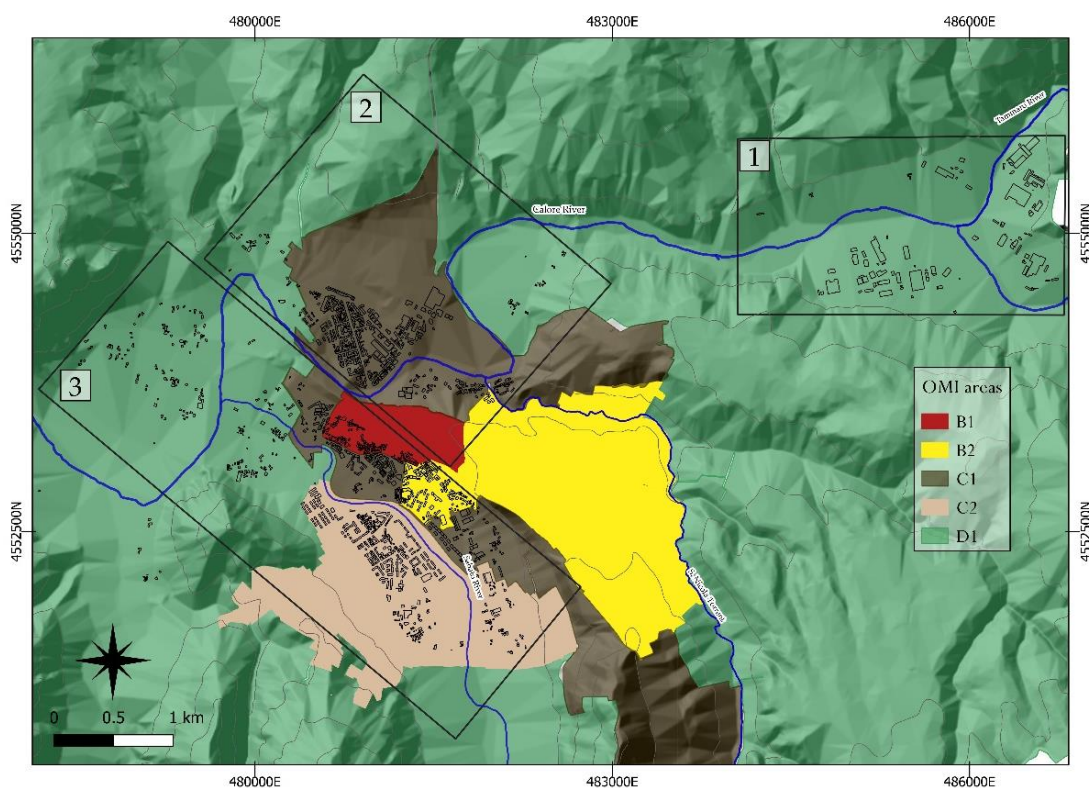


Figure 6. Map of Benevento’s buildings (black polygons) selected for the analysis and zonation of the OMI (Real Estate Market Observatory) areas. (B1) central area/historic center area; (B2) central urban area; (C1) semicentral urban area; (C2) semicentral/“Rione Libertà” area; (D1) suburban/agricultural area.

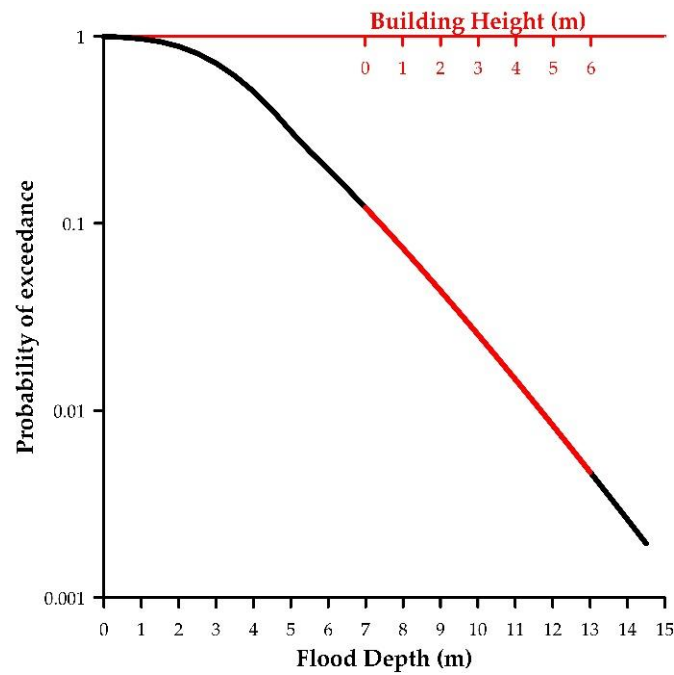


Figure 7. The generic flood hazard curve (black line) for the Benevento area compared with the height of a generic building (red line) located at a given position with respect to the watercourse and the hydrometric zero.

Figure 8a shows the vertical distribution of damage as a percentage of the economic value. It is assumed that each floor and its household and commercial contents has the same economic value but with some differences: (1) for structures with a surveyed cellar (only FAM dataset), 10% of the total value is given to the cellar, as it may contain perishable goods, as well as boilers, heating systems, and electrical systems; (2) for structures without a cellar or without cellar data (both FAM and DGM datasets), 10% extra is added to the first floor only to reduce possible underestimations.

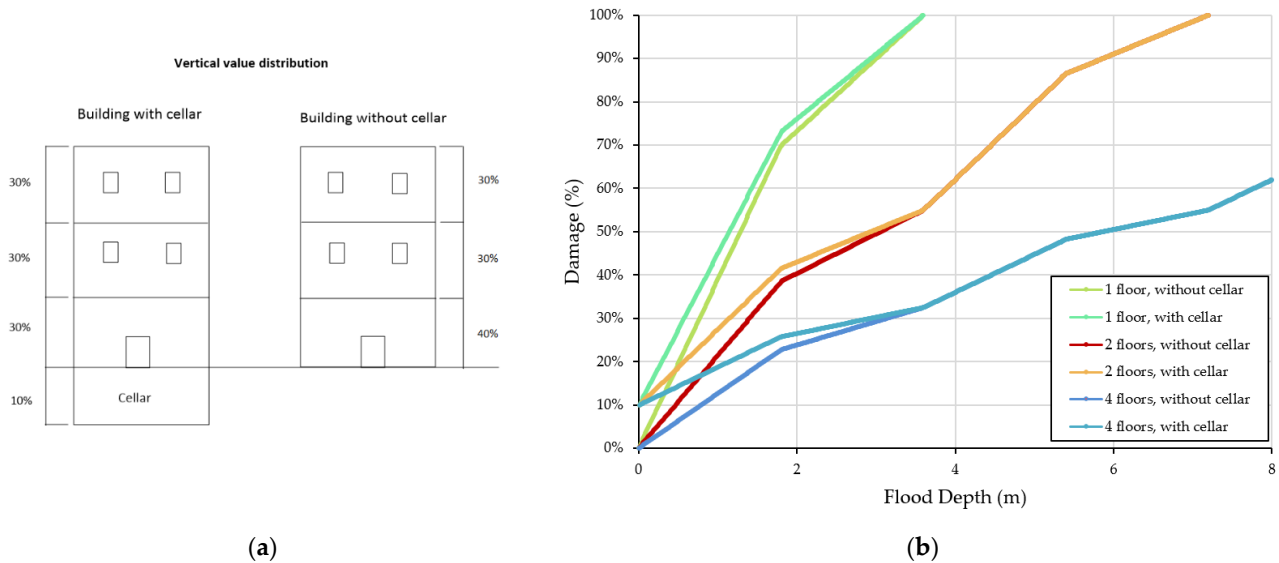


Figure 8. (a) Vertical distribution of the economic value for building with and without a cellar; (b) examples of stage–damage curves for buildings with different numbers of floors, with or without a cellar.

Figure 8b shows the stage–damage (%) curves created with the above assumption. Curves are derived for each type of 1–8-floor buildings, with and without a cellar. A loss of 70% of the economic value of each floor is assumed when water reaches the half floor; this assumption is consistent with the fact that most of the household contents and, in particular, electrical outlets are located in the lower part of the floors.

At this step of the analysis, the hazard curve of each single building is compared with the corresponding stage–damage curves in order to find the damage for each building and for each probability of exceedance (Figure 9).

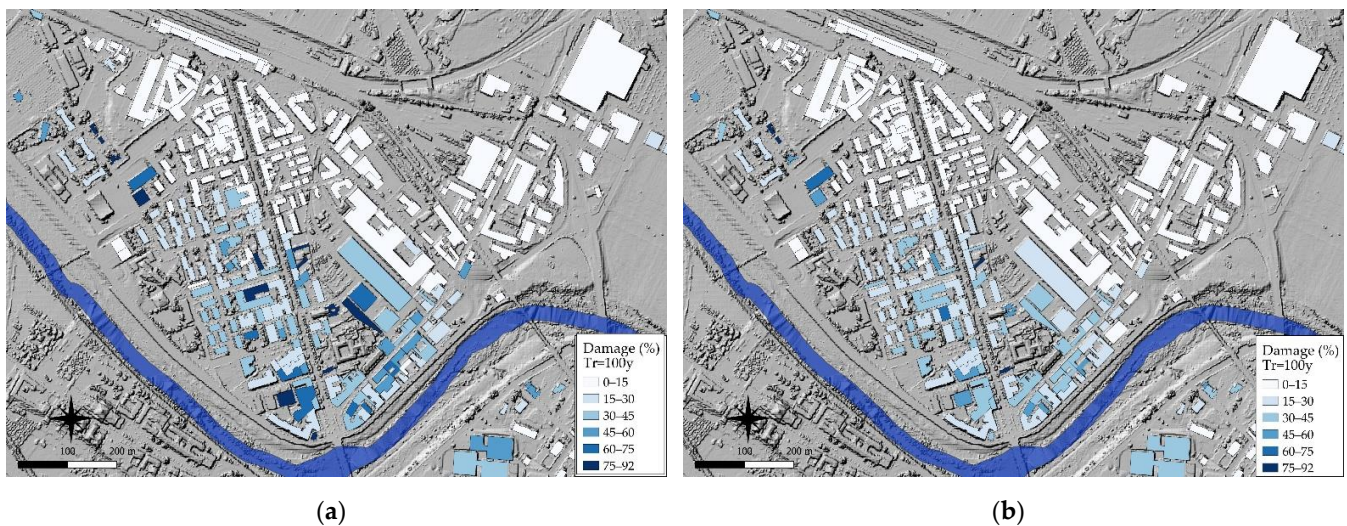


Figure 9. Example of damage degree (%) for buildings, considering their features extracted with FAM (a) and DGM (b) for a flood event with a return time (T_r) of 100 years.

3.4. Monetary Damage Estimate

After the application of the stage–damage function, the percentage losses are transformed into economic losses using Equations (6)–(8) and data from the revenue agency website (<https://www.agenziaentrate.gov.it/portale/> (accessed on 25 June 2018)) on the monetary value for each building category. The values for m^2 are calculated for each centimeter of height of the building; the total damage is then obtained by multiplying it by the total surface area.

As regards the vulnerability parameter c in Equation (7), the building type and maintenance status can have an important influence on the damage level suffered from flooding. For example, steel reinforced concrete buildings suffer less damage on the structural level compared to buildings made of other construction materials. As for other case studies of historical centers in Italy [25,27], buildings in the analyzed areas generally consist of ancient masonry edifices in the Rione Ferrovia and Rione Libertà areas, with a small percentage of prefabricated industrial warehouses. Therefore, during the flooding in October 2015, losses were mainly (1) nonstructural damage, which can be solved with major renovations (e.g., replacement of floors, painting, restoration of electrical and thermal systems, etc.) or (2) domestic and commercial contents damage. Based on these considerations, it is assumed that the vulnerability parameter c for nonstructural damage (1) can be defined from real estate valuations, taking into consideration the conservation state of the buildings and, more specifically, the relationship between the market value of a building in perfect condition and that of another that needs a thorough renovation. It was therefore assumed that $c = 0.2$ for structures as the ratio between the value of the two types of building is between 0.15 and 0.30 (Italian Revenue Agency). Conversely, the vulnerability parameter c for domestic and commercial contents (2) can be assumed to be 1 as their full replacement is expected after flooding.

Table 3 shows, instead, the correction factor (f in Equation (8)) for the estimation of the economic damage suffered by a household or commercial furniture in relation to the type of building. The value of the domestic contents is assessed according to a method proposed by the U.S. Hydrologic Engineering Center [58], which defines that value as a half percent of the value of the building for m^2 . Moreover, the correction factor f for commercial or industrial activities takes into account the fact that the commercial or industrial damage or destruction by flooding may have an economic value higher than that of the structure itself.

Table 3. Correction factor, f , for the evaluation of the economic damage suffered by a household or commercial furniture in relation to the cadastral category.

Types of Building	f ⁽¹⁾
Civil dwellings, economic housing, villas	0.50
Industrial sheds	3.50
Parking garages, boxes, shopping centers, stores, shops, offices, structured offices, laboratories, typical warehouses	2.00

⁽¹⁾ Equation (8).

3.5. Risk Assessment

The procedure for flood risk assessment was completed in a GIS environment. Different thematic data, organized in raster and vector information layers, are used in the QGIS platform. The following layers are used:

- Digital elevation model (DEM) and digital surface model (DSM) containing information about the territory;
- Water surface model and flood hazards;
- Layers of building types and characteristics: building identification number (GID), presence of cellar, number of floors, building height, building area, and type of building;
- Layers relating to the division of the OMI zones;
- Layers relating to stage–damage curves;
- Layers relating to the risk calculation.

Figures 10 and 11 show the flood risk maps of the study areas obtained by Equation (9) from FAM and DGM, respectively. The spatial distribution of economic losses, which is given per unit area per year (EUR/ m^2y), shows the direct correlation of the damage with the distance from the water course, even though it highlights a heterogeneity of results as a consequence of the different building type and characteristics.

In the absence of a cellar, the risk calculation for both methods are quite similar. In the Industrial area (sector 1, Figures 10 and 11), the economic value of the risk is matched exactly. A slightly higher variation occurs in the Rione Ferrovia area (sector 2, Figures 10 and 11), probably due to the fact that a large number of these buildings are characterized by a cellar, most of them being structures used as civil dwellings or offices. In the Rione Libertà area (sector 3, Figures 10 and 11), the risk value is visually higher than that obtained in the other quadrants. The higher unitary risk values are due to two main reasons: (1) the proximity to the watercourse and the high probability of being affected by flooding with shorter return times and, therefore, a higher probability of exceedance; (2) the morphological configuration, which is characterized by the minimum elevation difference of the area compared to the hydrometric zero of the watercourse. All these aspects constitute a condition of increased risk compared to the buildings located in the other sectors.

It should also be noted that, when estimating the unitary risk, all other conditions being equal, the number of floors influences the degree of damage: the more floors there are, the greater the risk value. On average, buildings of the Rione Libertà area are characterized by a higher number of floors than those of the other areas.

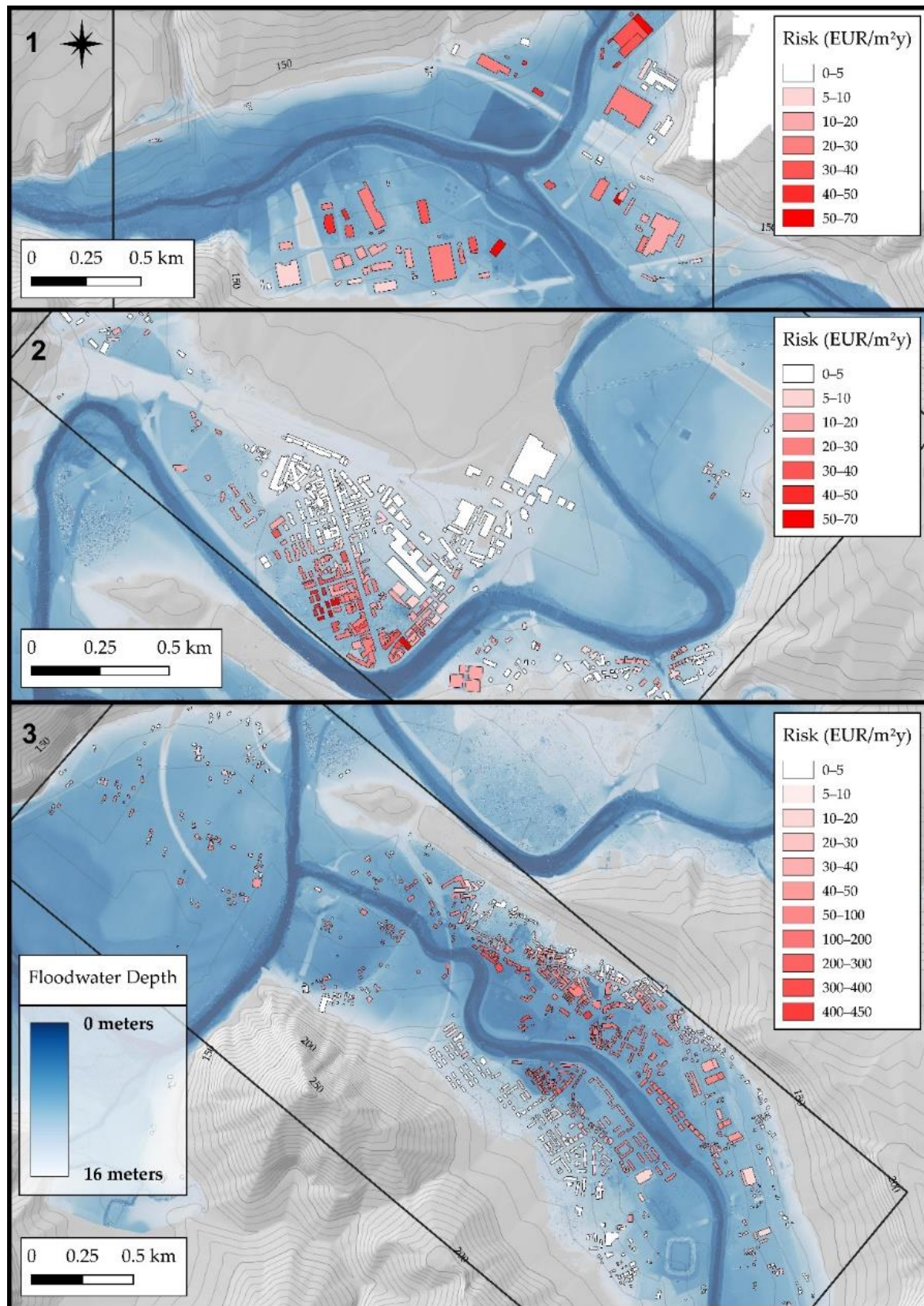


Figure 10. Flood risk maps (EUR/m²y) from FAM for Industrial area (1), Rione Ferrovia area (2), and Rione Libertà area (3).

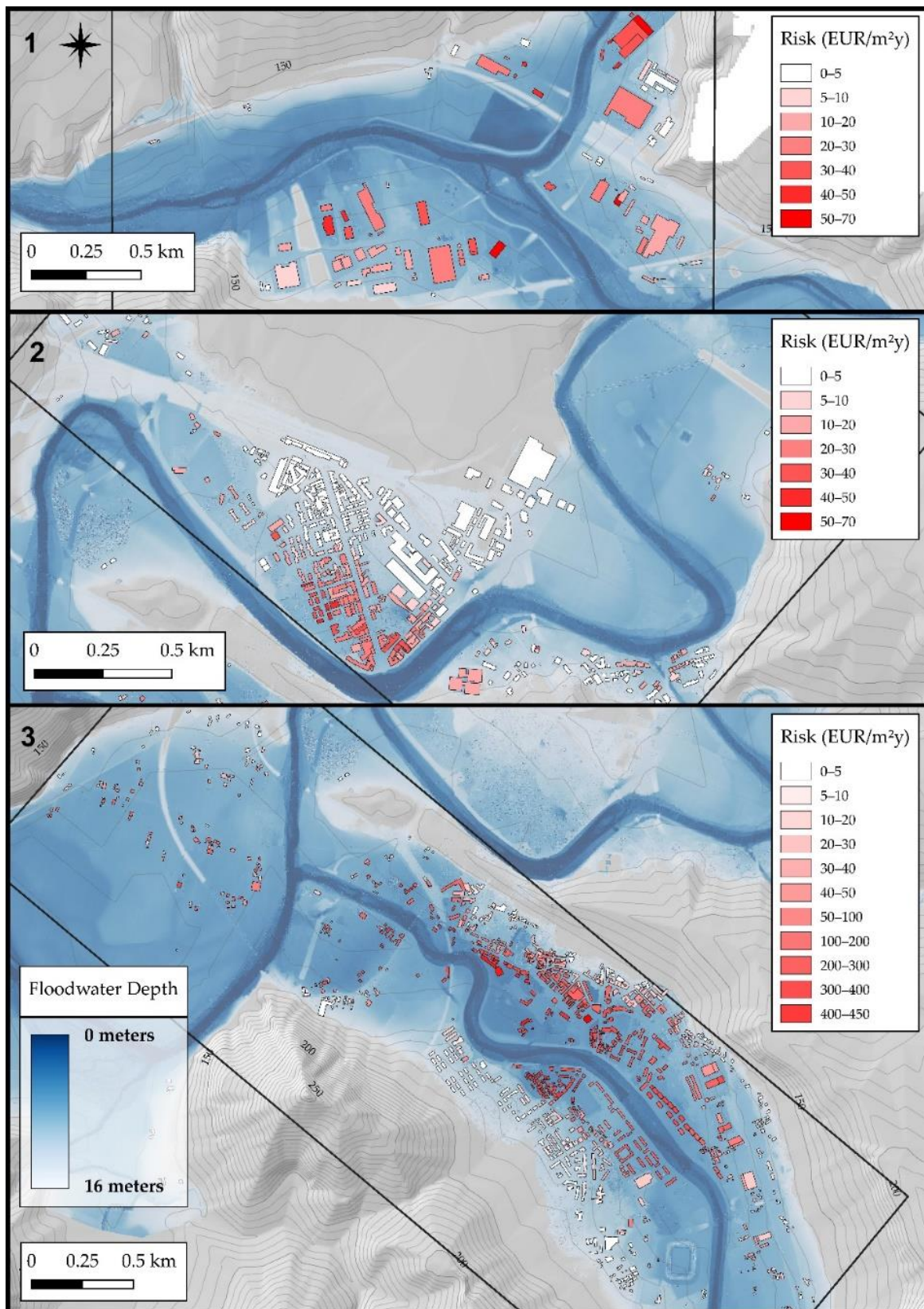


Figure 11. Flood risk maps (EUR/m²y) from DGM for Industrial area (1), Rione Ferrovia area (2), and Rione Libertà area (3).

4. Discussion

The analysis performed on flood risk evaluation at a microscale suggested that the two methods of data collection, FAM and DGM (Figure 12), led to very similar results in terms of loss per year, making the simplified approach the most efficient.

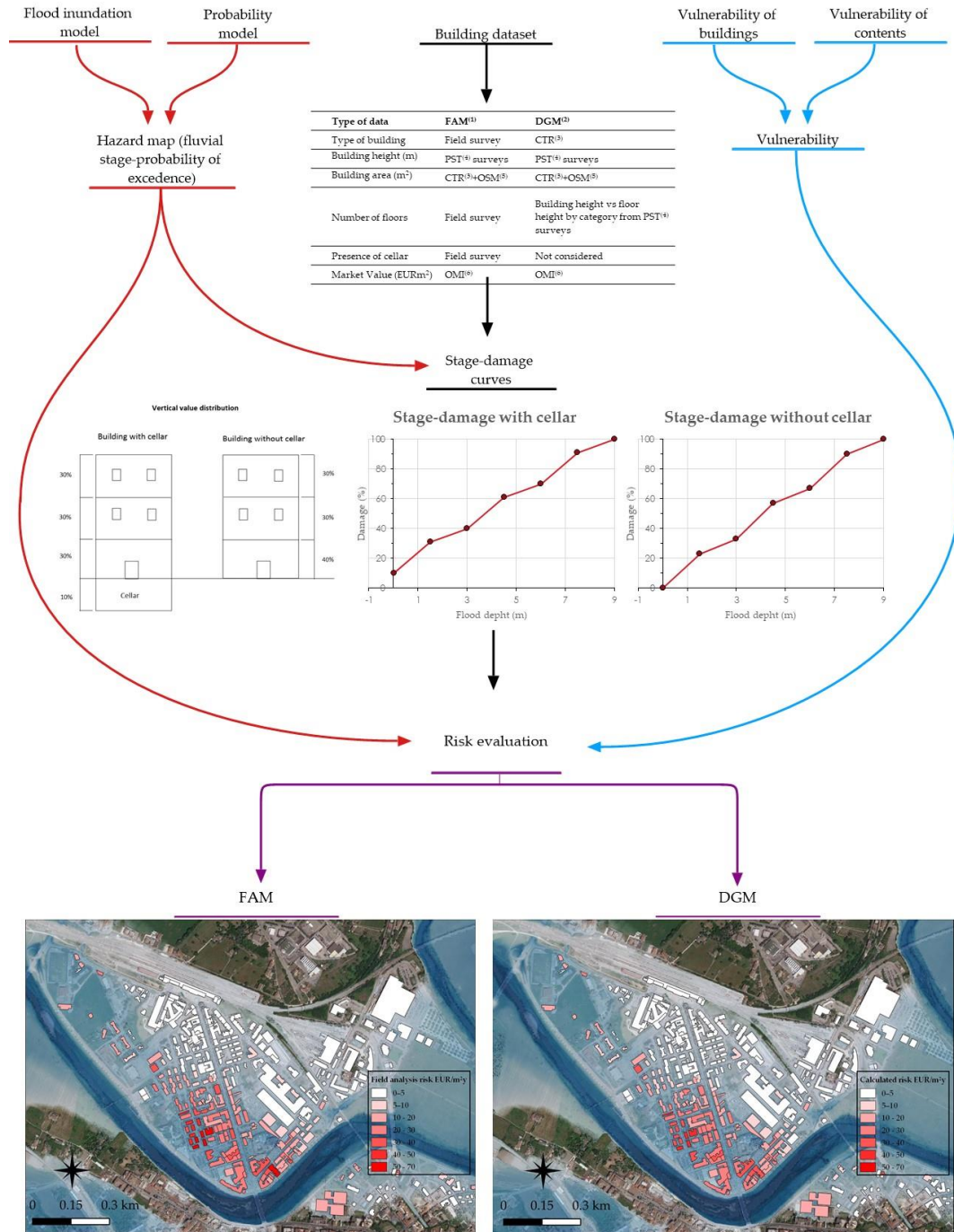


Figure 12. Conceptual model of the flood risk evaluation. See Table 1 and Figures 8, 10 and 11 for acronyms and legends.

Table 4 summarizes and compares the risk values obtained by using FAM and DGM. For all the analyzed buildings, the expected economic losses were about 29.35 and 28.36 million EUR/y, respectively, with a difference of 3.35% between the three sectors. In the Industrial area (sector 1, Figures 10 and 11), the difference in value was very low, due to the fact that the considered assets are mostly industrial storage facilities without

cellars. The most significant difference, about 10% of the estimated damage, was observed in the “Rione Ferrovia” area (sector 2, Figures 10 and 11), which consists mostly of dual-use ancient buildings (commercial activities on the ground floor and residential use on the upper floors) with cellars.

Table 4. Total damage (M EUR/y) for the study area and comparison between the different acquisition methods.

	FAM (M EUR/y)	DGM (M EUR/y)	Difference (%)
Total buildings	≈29.35	≈28.36	3.35
Industrial area	≈4.06	≈4.06	0.002
Rione Ferrovia area	≈1.97	≈1.75	10.36
Rione Libertà area	≈23.32	≈22.54	3.34

Table 5 shows the total damage comparison for each building category. Minor scattering of expected building damage was seen for FAM and DGM, except for civil dwellings and offices, which showed differences of 5.54% and 6.5%, respectively. Some other building categories exhibit null or negligible differences, thus the simplification adopted does not particularly affect the analysis outcome.

Table 5. Total damage (M EUR/y) for each building category and a comparison between the different acquisition methods.

Typology	Number of Buildings	FAM (M EUR/y)	DGM (M EUR/y)	Difference (%)
Total buildings	1533	≈29.35	≈28.36	3.35
Civil dwellings	893	≈14.59	≈13.78	5.54
Economic housing	94	≈0.49	≈0.48	0.76
Garages	12	≈0.76	≈0.73	2.80
Boxes	89	≈0.26	≈0.26	0.07
Villas	3	≈0.0037	≈0.0037	0.00
Shopping centers	5	≈0.13	≈0.12	2.72
Stores	21	≈1.06	≈1.06	0.00
Shops	67	≈4.30	≈4.29	0.15
Offices	60	≈2.19	≈1.98	6.50
Structured offices	4	≈0.15	≈0.15	0.00
Industrial sheds	149	≈4.63	≈4.63	0.02
Typical warehouses	125	≈0.27	≈0.27	0.00
Workshops	11	≈0.60	≈0.60	0.00

Table 6 only compares the expected economic damage between buildings with and without a basement, in order to evaluate underestimations of the simplified procedure. Elements without a basement, which are 1281 (about 84% of the analyzed assets), give similar values and the difference between accurate and generalized methods can be considered negligible. On the contrary, for the 252 buildings with a basement (about 16% of the analyzed assets), the modeled damage shows a large deviation (about 19.87%) between FAM and DGM, resulting in the cellar being the only factor influencing loss values in the comparative analysis between FAM and DGM. It should be noted that the 10% extra added to the first floor of structures without a cellar or without cellar data (see Section 3.3) only partially compensates for the absence of the data. This can be explained by taking into account that observation in European regions confirms that cellars and ground floors are more vulnerable and exposed to flooding than any other floor [59]. Therefore, even small flood depth can cause flooding of the cellars that lie below the road level.

Table 6. Total damage (M EUR/y) for buildings with and without a cellar.

Typology	Number of Buildings	FAM	DGM	Difference %
Without cellar	1281	≈22.34	≈22.34	0.0002
With cellar	252	≈4.94	≈3.96	19.87

5. Conclusions

In this paper, the flood risk across three sectors of the town of Benevento in southern Italy was evaluated, accounting for microscale risk estimation methods. The procedure, modified from that proposed by [27], considered direct and tangible damage as a function of the hydrometric height and allowed for quick estimates of the damage caused by alluvial events.

Data on the physical features of damageable buildings (e.g., number of floors, typology, presence of a basement) were analyzed by applying a simplified procedure of data generalization, which tries to overcome the limitations of the original method connected to the huge amounts of input data only obtainable by field surveys.

However, the two methods led to very similar results, with a difference of just 3.35% in estimating the total economic damage of 1533 buildings. This makes the generalized data acquisition method the most efficient as it responds to the need of reaching a reliable risk valuation in a shorter time. The limitations of the proposed analysis are related to the lack of information about the presence of cellars, which cannot be detected without field inspection.

Finally, the method described allows us to quickly assess the expected risk for any building as a result of a flood event of any specific intensity. This suggests that translating uncertainties into risk is also a matter of dealing with kairotic time, which shields failing economic frameworks from criticism [60]. As such, the method can represent a valid tool for the preliminary selection of sustainable measures concerning the management of the territory, such as limitations of use, planning and design of mitigation works, evacuation plans, increased awareness of risk among citizens, and the provision of support tools, such as insurance shields.

Author Contributions: Conceptualization, L.G., M.F., and P.R.; methodology, L.G., M.F. and G.M.; formal analysis, G.I.F., G.M. and S.R.; investigation, G.I.F.; data curation, G.I.F.; writing—original draft preparation, G.I.F., L.G., G.M., S.R. and P.R.; writing—review and editing, G.I.F., F.M.G. and P.R.; supervision, P.R.; project administration, P.R.; funding acquisition, F.M.G. and P.R. All authors have read and agreed to the published version of the manuscript.

Funding: This work was supported by the research funds of the University of Sannio and by SIGMA Project (Proof of Concept, D.D. n. 467 of 02.03.2018—Area: Smart Secure and Inclusive Communities—Code: POC01_00071—CUP: F84I19000630008).

Data Availability Statement: Not applicable.

Conflicts of Interest: The authors declare no conflict of interest.

References

1. Latour, B. Agency at the Time of the Anthropocene. *New Lit. Hist.* **2014**, *45*, 1–18. [[CrossRef](#)]
2. Lippert, I. *Latour's Gaia—Not down to Earth? Social Studies of Environmental Management for Grounded Understandings of the Politics of Human-Nature Relationships*; Institute for Advanced Studies on Science, Technology and Society: Graz, Austria, 2014. [[CrossRef](#)]
3. Domeneghetti, A.; Carisi, F.; Castellarin, A.; Brath, A. Evolution of Flood Risk over Large Areas: Quantitative Assessment for the Po River. *J. Hydrol.* **2015**, *527*, 809–823. [[CrossRef](#)]
4. Knox, J.C. Large Increases in Flood Magnitude in Response to Modest Changes in Climate. *Nature* **1993**, *361*, 430–432. [[CrossRef](#)]
5. Groisman, P.Y.; Knight, R.W.; Easterling, D.R.; Karl, T.R.; Hegerl, G.C.; Razuvaev, V.N. Trends in Intense Precipitation in the Climate Record. *J. Clim.* **2005**, *18*, 1326–1350. [[CrossRef](#)]
6. Dobler, C.; Bürger, G.; Stötter, J. Assessment of Climate Change Impacts on Flood Hazard Potential in the Alpine Lech Watershed. *J. Hydrol.* **2012**, *460–461*, 29–39. [[CrossRef](#)]

7. Kundzewicz, Z.W.; Ulbrich, U.; Brücher, T.; Graczyk, D.; Krüger, A.; Leckebusch, G.C.; Menzel, L.; Pińskwar, I.; Radziejewski, M.; Szwed, M. Summer Floods in Central Europe—Climate Change Track? *Nat. Hazards* **2005**, *36*, 165–189. [[CrossRef](#)]
8. Elmer, F.; Hoymann, J.; Duethmann, D.; Vorogushyn, S.; Kreibich, H. Drivers of Flood Risk Change in Residential Areas. *Nat. Hazards Earth Syst. Sci.* **2012**, *12*, 1641–1657. [[CrossRef](#)]
9. Gu, C.; Mu, X.; Gao, P.; Zhao, G.; Sun, W.; Li, P. Effects of Climate Change and Human Activities on Runoff and Sediment Inputs of the Largest Freshwater Lake in China, Poyang Lake. *Hydrol. Sci. J.* **2017**, *62*, 2313–2330. [[CrossRef](#)]
10. Wei, X.; Cai, S.; Ni, P.; Zhan, W. Impacts of Climate Change and Human Activities on the Water Discharge and Sediment Load of the Pearl River, Southern China. *Sci. Rep.* **2020**, *10*, 16743. [[CrossRef](#)]
11. Ruzza, G.; Guerriero, L.; Grelle, G.; Guadagno, F.M.; Revellino, P. Multi-Method Tracking of Monsoon Floods Using Sentinel-1 Imagery. *Water* **2019**, *11*, 2289. [[CrossRef](#)]
12. Bentivenga, M.; Giano, S.I.; Piccarreta, M. Recent Increase of Flood Frequency in the Ionian Belt of Basilicata Region, Southern Italy: Human or Climatic Changes? *Water* **2020**, *12*, 2062. [[CrossRef](#)]
13. Mandarino, A.; Luino, F.; Faccini, F. Flood-Induced Ground Effects and Flood-Water Dynamics for Hydro-Geomorphologic Hazard Assessment: The 21–22 October 2019 Extreme Flood along the Lower Orba River (Alessandria, NW Italy). *J. Maps* **2021**, *17*, 136–151. [[CrossRef](#)]
14. Malota, M.; Mchenga, J. Revisiting Dominant Practices in Floodwater Harvesting Systems: Making Flood Events Worth Their Occurrence in Flood-Prone Areas. *Appl. Water Sci.* **2020**, *10*, 6. [[CrossRef](#)]
15. Mazzorana, B.; Simoni, S.; Scherer, C.; Gems, B.; Fuchs, S.; Keiler, M. A Physical Approach on Flood Risk Vulnerability of Buildings. *Hydrol. Earth Syst. Sci.* **2014**, *18*, 3817–3836. [[CrossRef](#)]
16. Bermúdez, M.; Zischg, A.P. Sensitivity of Flood Loss Estimates to Building Representation and Flow Depth Attribution Methods in Micro-Scale Flood Modelling. *Nat. Hazards* **2018**, *92*, 1633–1648. [[CrossRef](#)]
17. Milanese, L.; Pilotti, M.; Belleri, A.; Marini, A.; Fuchs, S. Vulnerability to Flash Floods: A Simplified Structural Model for Masonry Buildings. *Water Resour. Res.* **2018**, *54*, 7177–7197. [[CrossRef](#)]
18. Cevasco, A.; Diodato, N.; Revellino, P.; Fiorillo, F.; Grelle, G.; Guadagno, F.M. Storminess and Geo-Hydrological Events Affecting Small Coastal Basins in a Terraced Mediterranean Environment. *Sci. Total Environ.* **2015**, *532*, 208–219. [[CrossRef](#)]
19. Costabile, P.; Costanzo, C.; De Lorenzo, G.; Macchione, F. Is Local Flood Hazard Assessment in Urban Areas Significantly Influenced by the Physical Complexity of the Hydrodynamic Inundation Model? *J. Hydrol.* **2020**, *580*, 124231. [[CrossRef](#)]
20. Ramos, H.M.; Besharat, M. Urban Flood Risk and Economic Viability Analyses of a Smart Sustainable Drainage System. *Sustainability* **2021**, *13*, 13889. [[CrossRef](#)]
21. Burgess, C.P.; Taylor, M.A.; Stephenson, T.; Mandal, A.; Powell, L. A Macro-Scale Flood Risk Model for Jamaica with Impact of Climate Variability. *Nat. Hazards* **2015**, *78*, 231–256. [[CrossRef](#)]
22. De Risi, R.; Jalayer, F.; De Paola, F. Meso-Scale Hazard Zoning of Potentially Flood Prone Areas. *J. Hydrol.* **2015**, *527*, 316–325. [[CrossRef](#)]
23. Kreibich, H.; Schröter, K.; Merz, B. Up-Scaling of Multi-Variable Flood Loss Models from Objects to Land Use Units at the Meso-Scale. *Proc. IAHS* **2016**, *373*, 179–182. [[CrossRef](#)]
24. Genovese, E. *A Methodological Approach to Land Use-Based Flood Damage Assessment in Urban Areas: Prague Case Study*; Technical EUR Reports; EUR: Luxembourg, 2006.
25. Oliveri, E.; Santoro, M. Estimation of Urban Structural Flood Damages: The Case Study of Palermo. *Urban Water* **2000**, *3*, 223–234. [[CrossRef](#)]
26. Ernst, J.; Dewals, B.; Detrembleur, S.; Archambeau, P.; Erpicum, S.; Piroton, M. Micro-Scale Flood Risk Analysis Based on Detailed 2D Hydraulic Modelling and High Resolution Geographic Data. *Nat. Hazards* **2010**, *55*, 181–209. [[CrossRef](#)]
27. Arrighi, C.; Brugioni, M.; Castelli, F.; Franceschini, S.; Mazzanti, B. Urban Micro-Scale Flood Risk Estimation with Parsimonious Hydraulic Modelling and Census Data. *Nat. Hazards Earth Syst. Sci.* **2013**, *13*, 1375–1391. [[CrossRef](#)]
28. Hasanzadeh Nafari, R.; Amadio, M.; Ngo, T.; Mysiak, J. Flood Loss Modelling with FLF-IT: A New Flood Loss Function for Italian Residential Structures. *Nat. Hazards Earth Syst. Sci.* **2017**, *17*, 1047–1059. [[CrossRef](#)]
29. Diodato, N. Ricostruzione storica di eventi naturali estrema carattere idrometeorologico nel sannio beneventanodal medioevo al 1998. *Boll. Geofis.* **1999**, *22*, 5–39.
30. Diodato, N. Climatic Fluctuations in Southern Italy since the 17th Century: Reconstruction with Precipitation Records at Benevento. *Clim. Change* **2007**, *80*, 411–431. [[CrossRef](#)]
31. Santo, A.; Santangelo, N.; Forte, G.; De Falco, M. Post Flash Flood Survey: The 14th and 15th October 2015 Event in the Paupisi-Solopaca Area (Southern Italy). *J. Maps* **2017**, *13*, 19–25. [[CrossRef](#)]
32. Revellino, P.; Guerriero, L.; Mascellaro, N.; Fiorillo, F.; Grelle, G.; Ruzza, G.; Guadagno, F.M. Multiple Effects of Intense Meteorological Events in the Benevento Province, Southern Italy. *Water* **2019**, *11*, 1560. [[CrossRef](#)]
33. Guerriero, L.; Focareta, M.; Fusco, G.; Rabuano, R.; Guadagno, F.M.; Revellino, P. Flood Hazard of Major River Segments, Benevento Province, Southern Italy. *J. Maps* **2018**, *14*, 597–606. [[CrossRef](#)]
34. Guerriero, L.; Ruzza, G.; Calcaterra, D.; Di Martire, D.; Guadagno, F.M.; Revellino, P. Modelling Prospective Flood Hazard in a Changing Climate, Benevento Province, Southern Italy. *Water* **2020**, *12*, 2405. [[CrossRef](#)]

35. Grelle, G.; Rossi, A.; Revellino, P.; Guerriero, L.; Guadagno, F.M.; Sappa, G. Assessment of Debris-Flow Erosion and Deposit Areas by Morphometric Analysis and a GIS-Based Simplified Procedure: A Case Study of Paupisi in the Southern Apennines. *Sustainability* **2019**, *11*, 2382. [CrossRef]
36. Magliulo, P.; Valente, A. GIS-Based Geomorphological Map of the Calore River Floodplain Near Benevento (Southern Italy) Overflooded by the 15th October 2015 Event. *Water* **2020**, *12*, 148. [CrossRef]
37. Zazo, A. Lo straripamento del fiume Calore in Benevento nel 1740 e nel 1770. *Sannium* **1949**, *3–4*, 212.
38. Andriola, L.; Delmonaco, G.; Margottini, C.; Serafini, S.; Trocciola, A. Andamenti Meteoclimatici Ed Eventi Naturali Estremi in Italia Negli Ultimi 1000 Anni: Alcune Esperienze Nell' ENEA. *Atti Dei Convegni Lincei-Accad. Naz. Dei Lincei* **1995**, *129*, 95–116.
39. Cardinali, M.; Cipolla, F.; Guzzetti, F.; Lolli, O.; Pagliacci, S.; Reichenbach, P.; Tonelli, G. *Catalogo Delle Informazioni Sulle Località Italiane Colpite Da Frane e Di Inondazioni*; Consiglio nazionale delle ricerche: Rome, Italy, 1998.
40. Rossi, F.; Villani, P. Valutazione Delle Piene in Campania; Rapporto Regionale Campania; CNR-GNDCI. 1994. Available online: http://www.gndci.cnr.it/it/vapi/welcome_it.htm (accessed on 1 May 2018).
41. Diodato, N.; Soriano, M.; Bellocchi, G.; Fiorillo, F.; Cevasco, A.; Revellino, P.; Guadagno, F.M. Historical Evolution of Slope Instability in the Calore River Basin, Southern Italy. *Geomorphology* **2017**, *282*, 74–84. [CrossRef]
42. Office of the United Nations Disaster Relief Coordinator. Natural Disasters and Vulnerability Analysis. 1980. Available online: <https://digitallibrary.un.org/record/95986> (accessed on 1 September 2017).
43. Varnes, D.J.; IAEG Commission. *Landslide hazard zonation: A review of principles and practice*; UNESCO Press: Paris, France, 1984; 63p.
44. Uddin, K.; Matin, M.A. Potential Flood Hazard Zonation and Flood Shelter Suitability Mapping for Disaster Risk Mitigation in Bangladesh Using Geospatial Technology. *Prog. Disaster Sci.* **2021**, *11*, 100185. [CrossRef]
45. Guerriero, L.; Ruzza, G.; Guadagno, F.M.; Revellino, P. Flood Hazard Mapping Incorporating Multiple Probability Models. *J. Hydrol.* **2020**, *587*, 125020. [CrossRef]
46. Montané, A.; Buffin-Bélanger, T.; Vinet, F.; Vento, O. Mappings Extreme Floods with Numerical Floodplain Models (NFM) in France. *Appl. Geogr.* **2017**, *80*, 15–22. [CrossRef]
47. Scorpio, V.; Roskopf, C.M. Channel Adjustments in a Mediterranean River over the Last 150 Years in the Context of Anthropogenic and Natural Controls. *Geomorphology* **2016**, *275*, 90–104. [CrossRef]
48. Sutcliffe, J.V. The Use of Historical Records in Flood Frequency Analysis. *J. Hydrol.* **1987**, *96*, 159–171. [CrossRef]
49. Woo, M.; Waylen, P.R. Probability Studies of Floods. *Appl. Geogr.* **1986**, *6*, 185–195. [CrossRef]
50. Hosking, J.R.M.; Wallis, J.R. The Value of Historical Data in Flood Frequency Analysis. *Water Resour. Res.* **1986**, *22*, 1606–1612. [CrossRef]
51. Yue, S. A Bivariate Gamma Distribution for Use in Multivariate Flood Frequency Analysis. *Hydrol. Processes* **2001**, *15*, 1033–1045. [CrossRef]
52. Mojtahedi, M.; Oo, B.L. Built Infrastructure Conditions Mediate the Relationship between Stakeholders Attributes and Flood Damage: An Empirical Case Study. *Sustainability* **2021**, *13*, 9739. [CrossRef]
53. Agenzia Delle Entrate: Sintesi Degli Studi Di Settore. Available online: <https://www.agenziaentrate.gov.it/portale/web/guest/archivio/archivoschedeadempimento/schede-adempimento-2018/dichiarazioni/studisettore> (accessed on 25 June 2018).
54. Kang, J.-L.; Su, M.-D.; Chang, L.-F. Loss functions and framework for regional flood damage estimation in residential area. *J. Mar. Sci. Technol.* **2005**, *13*, 5. [CrossRef]
55. Luino, F.; Cirio, C.G.; Biddoccu, M.; Agangi, A.; Giulietto, W.; Godone, F.; Nigrelli, G. Application of a Model to the Evaluation of Flood Damage. *Geoinformatica* **2009**, *13*, 339–353. [CrossRef]
56. Jordan, S.; Jørgensen, L.; Mitterhofer, H. Performing Risk and the Project: Risk Maps as Mediating Instruments. *Manag. Account. Res.* **2013**, *24*, 156–174. [CrossRef]
57. Kalthoff, H. Practices of Calculation: Economic Representations and Risk Management. *Theory Cult. Soc.* **2005**, *22*, 69–97. [CrossRef]
58. US Army corpsHydrologic Engineerin Center HEC-FIA Flood Impact Analysis, User's Manual. Available online: https://www.hec.usace.army.mil/software/hec-fia/documentation/HEC-FIA_30_Users_Manual.pdf (accessed on 25 June 2018).
59. Karagiorgos, K.; Thaler, T.; Hübl, J.; Maris, F.; Fuchs, S. Multi-Vulnerability Analysis for Flash Flood Risk Management. *Nat. Hazards* **2016**, *82*, 63–87. [CrossRef]
60. Themsen, T.N.; Skærbæk, P. The Performativity of Risk Management Frameworks and Technologies: The Translation of Uncertainties into Pure and Impure Risks. *Account. Organ. Soc.* **2018**, *67*, 20–33. [CrossRef]